

REPORT DOCUMENTATION PAGE				Form Approved OMB No. 0704-0188	
Public reporting burden for this collection of information is estimated to average 1 hour per response, including the time for reviewing instructions, searching existing data sources, gathering and maintaining the data needed, and completing and reviewing the collection of information. Send comments regarding this burden estimate or any other aspect of this collection of information, including suggestions for reducing the burden, to Department of Defense, Washington Headquarters Services, Directorate for Information Operations and Reports (0704-0188), 1215 Jefferson Davis Highway, Suite 1204, Arlington, VA 22202-4302. Respondents should be aware that notwithstanding any other provision of law, no person shall be subject to any penalty for failing to comply with a collection of information if it does not display a currently valid OMB control number. PLEASE DO NOT RETURN YOUR FORM TO THE ABOVE ADDRESS.					
1. REPORT DATE (DD-MM-YYYY) 21-12-2004		2. REPORT TYPE Final Report		3. DATES COVERED (From – To) 4 March 2003 - 04-Jan -05	
4. TITLE AND SUBTITLE Detection and Characterization of Phase-Coded Radar Signals			5a. CONTRACT NUMBER FA8655-03-1-3030		
			5b. GRANT NUMBER		
			5c. PROGRAM ELEMENT NUMBER		
6. AUTHOR(S) Dr. Ernest R. Adams			5d. PROJECT NUMBER		
			5d. TASK NUMBER		
			5e. WORK UNIT NUMBER		
7. PERFORMING ORGANIZATION NAME(S) AND ADDRESS(ES) Cranfield University (RMCS) Shrivenham SN6 8LA United Kingdom				8. PERFORMING ORGANIZATION REPORT NUMBER N/A	
9. SPONSORING/MONITORING AGENCY NAME(S) AND ADDRESS(ES) EOARD PSC 802 BOX 14 FPO 09499-0014				10. SPONSOR/MONITOR'S ACRONYM(S)	
				11. SPONSOR/MONITOR'S REPORT NUMBER(S) SPC 03-3030	
12. DISTRIBUTION/AVAILABILITY STATEMENT Approved for public release; distribution is unlimited.					
13. SUPPLEMENTARY NOTES					
14. ABSTRACT This report results from a contract tasking Cranfield University (RMCS) as follows: The Grantee will investigate various mathematical concepts of detection and characterization of simulated radar signals. As detailed in the technical proposal, at least four approaches will be investigated: 1. A varied matched filter and spectral analysis. 2. A neural network (NN) approach, based on the use of NNs to detect pulse radar. 3. Methods derived from CDMA (code division multiple access) multiuser detection. 4. Independent component analysis (ICA). He will employ MATLAB and SIMULINK to generate signals and MATLAB for their analysis. Efficiency of algorithms will be an important consideration in assessing the performance of the mathematical approaches developed.					
15. SUBJECT TERMS EOARD, Signal Processing, radar					
16. SECURITY CLASSIFICATION OF:			17. LIMITATION OF ABSTRACT UL	18. NUMBER OF PAGES 21	19a. NAME OF RESPONSIBLE PERSON PAUL LOSIEWICZ, Ph. D.
a. REPORT UNCLAS	b. ABSTRACT UNCLAS	c. THIS PAGE UNCLAS			19b. TELEPHONE NUMBER (Include area code) +44 20 7514 4474

CONTRACT TITLE: **Detection and Characterization of Phase-coded Radar Signals**

SPONSOR: **AFRL/SNRP, WPAFB through EOARD, London**

SPONSOR'S REFERENCE: **033030**

FINAL REPORT: **Research carried out up to December 2004 by Dr E R Adams, Cranfield University (RMCS)**

1. **Summary**

Relatively simple correlation/matched filter techniques were developed to detect and identify phase-coded radar signals based on true Barker codes and longer, combined Barker codes. Detection and identification rates were good, though not so good as those possible with more sophisticated techniques like neural networks. However, the simplicity and computational efficiency of the new methods make them worthwhile for some applications.

2. **Description of the problem**

The problem is to detect and characterize pulsed phase-coded radar signals in noise. Gaussian noise is assumed, although further work would consider non-Gaussian noise and interference from DS/SS-based CDMA transmissions. Partial knowledge of the radar signal is assumed, in particular the carrier frequency and the type of pseudo-random sequence used to determine phase. Barker codes are investigated first but, as the longest known true Barker code is only 13 bits and short codes require high power levels for a given energy, longer codes created from true Barker codes are also considered. The extended problem of detecting multi-phase Barker codes, other pseudo-random codes like m-sequences and forms of wideband interrupted CW was not attempted.

3. Properties of phase-coded radar signals

A medium/long-range surveillance radar typically requires a range resolution ΔR of 15 m. This ΔR implies a waveform RF bandwidth B of 10 MHz. From Gabor's theorem, bit duration is $1/B = 10^{-7}$ s. Assuming the 13-bit Barker code, the pulse in Figure 1 results.

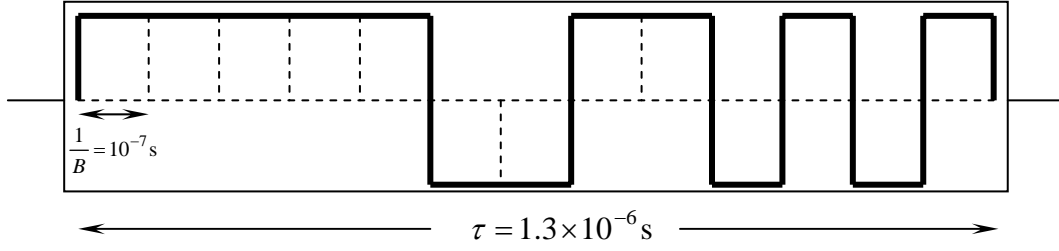


Figure 3.1: Radar pulse for a 13-bit Barker code

Time delay t_d is related to range-to-target R by the equation

$$ct_d = 2R \Rightarrow t_d = \frac{2R}{c}, \quad (3.1)$$

so time-delay resolution Δt_d is related to range resolution ΔR by the equation:

$$\Delta t_d = \frac{2\Delta R}{c} \Rightarrow \Delta R = \frac{c\Delta t_d}{2} \quad (3.2)$$

But Δt_d is known to be $1/B$, giving range resolution

$$\Delta R = \frac{c\Delta t_d}{2} = \frac{c}{2B} \quad (3.3)$$

Thus $B = 10$ MHz gives the desired range resolution of 15 m. Pulse duration τ results from the choice of the 13-bit Barker code.

The pulse-repetition interval T , illustrated in Figure 3.2, is a more fundamental variable than τ . It is determined by the maximum unambiguous range, R_u :

$$T = \frac{2R_u}{c} \quad (3.4)$$

τ should then be chosen to satisfy $3\tau \leq T$ in order to avoid eclipsing. In practice, for short pulses like the 13-bit Barker code, $T \gg 3\tau$. Greater efficiency results (power reduced) if τ approaches $T/3$ ($\tau = T$ produces CW), which provides the motivation for examining the longer codes in section 6.

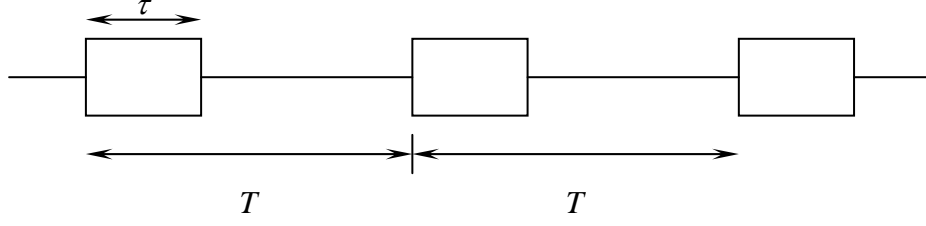


Figure 3.2: Train of regularly repeating pulses

The length of the pulse train is $t_0 = nT$, i.e. the train has n pulses. The variable n is determined by the requirement that $2E/N_0$ at maximum range must be 20 dB, where $E = S\tau$, S being signal power. This may alternatively be stated in the relation between output and input SNRs:

$$\frac{2E}{N_0} = 2n(B\tau) \left[\frac{S}{N} \right], \quad (3.5)$$

i.e. $2nB\tau$ is the integration improvement factor.

Finally, T_s is the interval between pulse trains, satisfying:

$$T_s = \frac{\Omega}{\Omega_b} t_0 \quad (3.6)$$

where Ω is the solid angle of search and Ω_b is the solid angle of the radar beam. In practice, the choice of T_s is more arbitrary than for other parameters. In simulations, T_s was initially assumed to be constant. Later, it was assumed to be uniformly distributed between $T_s - t_0/2$ and $T_s + t_0/2$.

The following values were used in initial simulations:

$$B = 10 \text{ MHz}, \quad \frac{1}{B} \text{ (bit length)} = 10^{-7} \text{ s}$$

$$\tau = 1.3 \times 10^{-6} \text{ s (for 13-bit Barker code)}$$

$$\tau = m \times 10^{-7} \text{ s for pseudo-random } m\text{-bit code}$$

$$T = 7 \times 10^{-4} \text{ s, based on } R_u = 100 \text{ km, } T = \frac{2R_u}{c}$$

$$n = 20 \Rightarrow t_0 = nT = 1.4 \times 10^{-2} \text{ s}$$

$$T_s = 3 \text{ s (constant)}$$

$T_s = 3 + (\text{rand} - 0.5)t_0$, where rand is the Matlab function returning a uniformly distributed value between 0 and 1.

4. Barker and other pseudo-random codes for phase coding

4.1 True Barker codes

The nine known Barker codes are represented in Table 4.1.

Length N	c_n
2	++
2	-+
3	++-
4	++-+
4	+++ -
5	++++ - +
7	++++ - - + -
11	++++ - - - + - - + -
13	++++ + - - + + - + - +

Table 4.1: Barker codes

Barker codes have autocorrelation functions (ACFs) with equal time sidelobes: they are the only codes for which ACF sidelobes at zero Doppler have levels $\leq N$ (code length). As explained in section 2, they are too short for some applications – the greatest sidelobe reduction, for $N = 13$, is -22.3 dB. However it is possible to combine Barker codes to create longer codes with good properties.

4.2 Combined Barker codes

This method involves phase coding with one Barker code within each segment of another Barker code. For example, the Barker code of length 3, B_3 , may be combined with that of length 5, B_5 , to create a code of length 15 (Figure 4.1):

$$B_{53} = (++++-, +++-+, ---+-) \quad (4.1)$$

Note that B_{nm} is the Kronecker product $B_n \otimes B_m$, regarding sequences as row vectors.

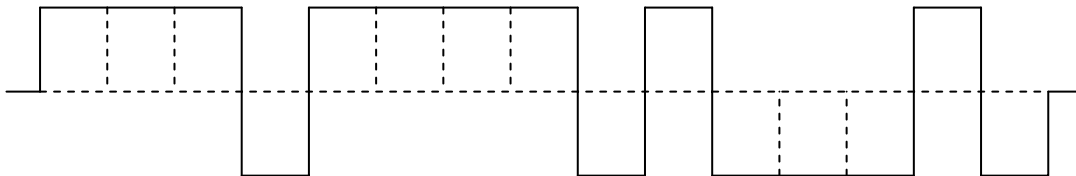


Figure 4.1: Combined Barker Code B_{53}

The order in which the two codes are combined is significant, i.e. $B_{n,m} \neq B_{m,n}$. [1,2] give examples of the different code properties of the alternative orderings. E.g. $B_{4,13}$, for which each bit of the 13-bit code B_{13} is coded into four bits, has a zero Doppler ACF with four side peaks of amplitude 13 at shifts ± 1 and ± 3 , and 12 peaks of amplitude 4. $B_{13,4}$ has the same number of side peaks of amplitude > 1 , but the side

peaks of amplitude 13 occur at shifts of ± 13 and ± 39 . The main peak of the ACF in both cases has amplitude 52. $B_{4,13}$ is useful if expected interference is well separated in range from the target.

Combining pairs of Barker codes simply in this way can give codes up to $11 \times 13 = 143$ bits long. The properties of 3-way combinations, e.g. $3 \times 5 \times 7$, are not known. Note that B_{nn} is not used because of high partial correlations.

4.3 **n-Phase Barker codes**

n -phase Barker sequences, e.g. using phase alphabets such as multiples of $\pi/6$, are defined and their properties explored in [3,4]. They will be investigated if time allows.

5. Methods for detection and characterization of Barker sequences

5.1 Correlation/pattern recognition techniques

These newly developed techniques begin with calculating the ACF of a length T_p of signal, where $T_p > nT$, the highest reasonable value of the unknown nT , and $T_p \ll T_s$, i.e. T_p is selected so there is a high probability it will include a single pulse train of n pulses of length T . FFTs are used to estimate the ACF to improve efficiency. Figure 5.1 illustrates the ACF for a noiseless pulse train of B_3 pulses.

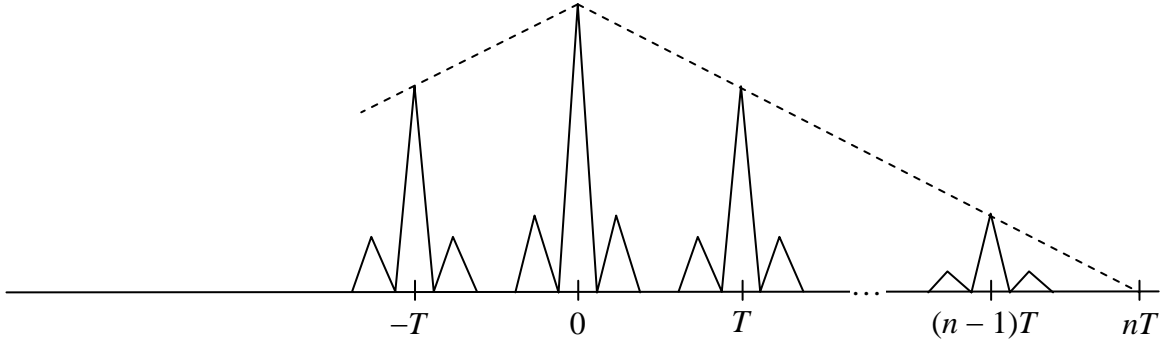


Figure 5.1: ACF of 3-length code

Pattern recognition algorithms are under development to recognize the repeating waveform, linearly decreasing in amplitude at multiples of $|T|$, with the aim of estimating T . Alternatively, pattern recognition may be carried out in the frequency domain. Assuming signal $x(t)$ is sampled at intervals of Δt , i.e. $x_i = x(i\Delta t)$, and $T = M\Delta t$, then the pulse train of n Barker codes b_i , $0 \leq i \leq N-1$, may be written:

$$y_i = b_i * \sum_{k=0}^{n-1} \delta(i - kM) \quad (5.1)$$

The DFT of the pulse train y_i is thus the product of the DFT of the Barker code with the DFT of the finite train of impulse functions. If $n \rightarrow \infty$, a line spectrum of the Barker code results, with spectral line spacing $1/T$ Hz. For finite n , this spectrum is convolved with $\text{sinc}(nTf)$, i.e. a very narrow sinc function with zeros at integer multiples of $1/nT$. Assuming $T = M\Delta t$ and $T_p = P\Delta t$, the frequency resolution of the FFT for window T_p is $1/P\Delta t$, so the spectral lines at $1/M\Delta t$ will be sampled only if M divides P . This is illustrated in Figure 5.2. Algorithms are being developed to estimate T from the DFT or power spectrum of x_i .

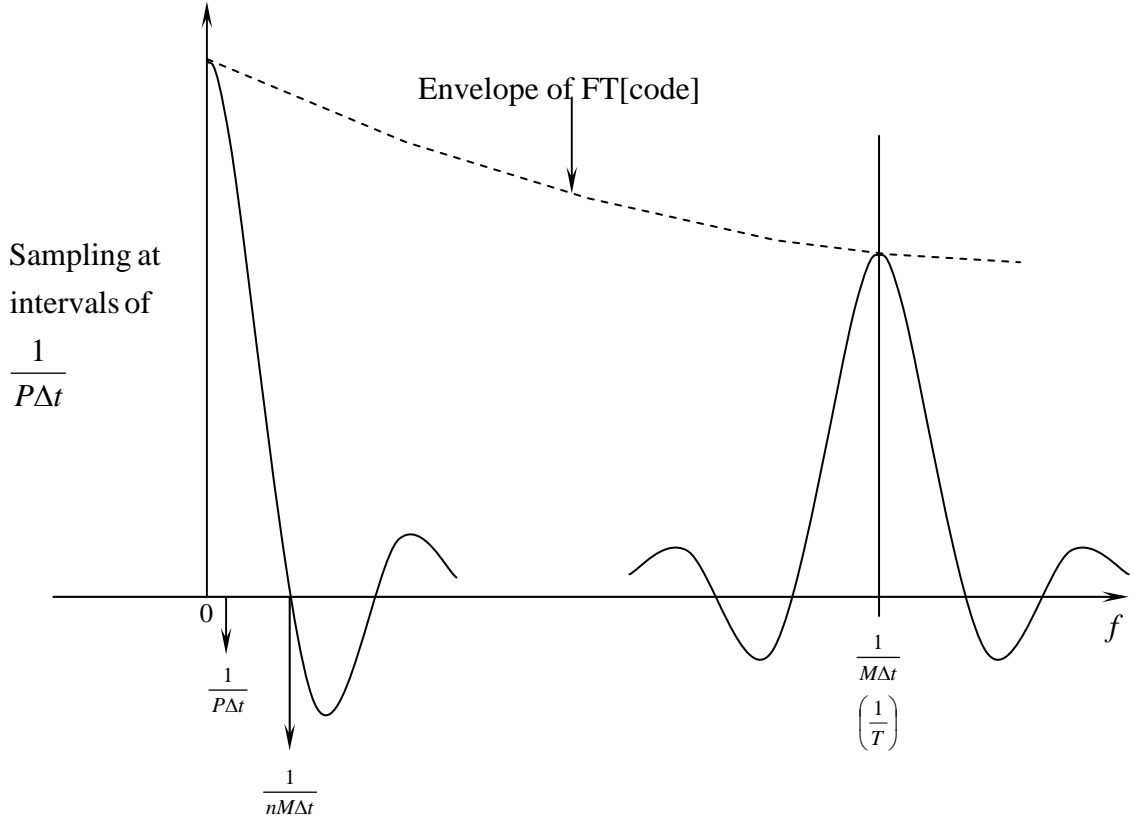


Figure 5.2: Fourier transform of signal with T_p -length window

The estimate \hat{T} , either from the ACF or FFT method, is used to identify the unknown waveform by dividing the interval T_a into K segments of length \hat{T} and averaging (K is the largest integer for which $K\hat{T} \leq T_a$). Assuming $\hat{T} = M'\Delta t$,

$$u_i = \frac{1}{K} \sum_{k=0}^{K-1} x_{i+kM'}, \quad 0 \leq i \leq M-1 \quad (5.2)$$

The averaging reduces noise and allows easier detection of the single Barker waveform in u_i with a matched filter or neural network.

5.2 Simulation results for correlation techniques

The performance of a combination of the techniques in 5.1 was assessed in initial simulations. To reduce computational effort, T was taken to be 7×10^{-5} s. Otherwise, the values in section 3 were used. A two-stage method detected the presence of a repeating pulse-waveform and estimated T , the pulse-repetition interval. Because of the high cost of ACF estimation, detection and initial estimation of T were based on the signal's Fourier spectrum. This allowed a more precise estimate of T , following detection and initial T estimation, from a narrow search of ACF values. The refined T estimate was then used to produce an averaged pulse-waveform, i.e. one with greatly reduced noise. The final stage was to identify the waveform by correlation with Barker codes – a matched filter approach. In more detail, the stages were:

(1) As described in 5.1, the DFT of a signal containing a repeating waveform consists of narrow sinc functions spaced at $1/T$ Hz intervals, the sinc amplitudes depending on the waveform's Fourier transform. The FFT X_k of the P -length signal (same symbols used as in 5.2) was used to test for repeating sinc functions by finding the value $i = r$ which maximizes

$$Y_i = \frac{X_i + X_{2i} + X_{3i} + \dots + X_{k_i i}}{k_i} \quad (5.3)$$

So

$$i \neq r \Rightarrow Y_r \geq Y_i \quad (5.4)$$

This Y_r was then tested against a threshold to detect the presence of a repeating waveform. If a repeating waveform was detected the following approximate estimate of T was calculated:

$$\hat{T}_1 = \frac{P\Delta t}{r} \quad (5.5)$$

The estimate is not exact as, in general, $1/T$ is not a sampled frequency of the FFT, i.e. the sinc functions' centres are not sampled.

Detection rates for B_{13} pulse-trains in alternative noise environments are given in table 5.2. False alarm rates, i.e. detection rates when no pulse-train is present, are also given.

(2) Given \hat{T}_1 from the first stage (5.5), a more accurate estimate of T (and one that may be exact) may be derived by examining ACF values for shifts close to \hat{T}_1 . For such a corresponding m , a shift index for which $m\Delta t \cong \hat{T}_1$, the ACF is

$$C_m = E[x_i x_{i+m}], \quad (5.6)$$

estimated by averaging $x_i x_{i+m}$ over all possible i ($1 \leq i \leq P - m$). For m values satisfying

$$|m\Delta t - \hat{T}_1| \leq \Delta T, \quad (5.7)$$

ΔT being determined by trial and error, the following statistic was maximized:

$$D_m = \frac{C_m + C_{2m} + C_{3m} + \dots + C_{k_m m}}{k_m} \quad (5.8)$$

For M' corresponding to this maximum, i.e.

$$m \neq M' \Rightarrow D_{M'} \geq D_m \quad (5.9)$$

the final estimate for T becomes:

$$\hat{T} = M'\Delta t \quad (5.10)$$

(3) \hat{T} was then used to produce a waveform with reduced noise by averaging signal segments of length \hat{T} (5.2). The waveform was identified by correlating the averaged segment with alternative Barker codes. A match was found if the maximum correlation exceeded a pre-determined threshold. Although only B_{13} signals were simulated, the averaged segment was also correlated with B_{11} and false detection rates (deciding B_{11} was present instead of the actual B_{13}) were estimated. Also estimated were failure rates to detect any pulse-train when B_{13} was present. The identification results may be seen in table 5.3. The confusion between B_{13} and B_{11} may be explained by their high cross-correlation:

$$\begin{aligned} CC_j(13,11) &= \sum_i B_{13}(i)B_{11}(i+j) \\ &= 0 \cdots 0 -1 \ 0 -1 -2 -1 \ 0 -3 -4 \ 1 \ 0 -3 \ 7 \ 3 \ 0 -1 -4 \ 3 \ 0 \ 1 -2 \ 1 \ 0 \ 1 \ 0 \cdots 0 \end{aligned} \quad (5.11)$$

More sophisticated pattern recognition algorithms are being developed to distinguish Barker codes. The cross-correlation properties of Barker codes are also under investigation.

Noise	% Detection	% False alarms
6 dB	96	2
3 dB	86	8
0 dB	62	42

Table 5.2: Detection/false alarm rates for B_{13}

Noise	% Identification (B_{13})	% False identification (B_{11})	% Failure to identify
6 dB	100	4	0
3 dB	98	12	0
0 dB	90	26	6

Table 5.3: Identification rates for B_{13}

Each estimated % in tables 5.2 and 5.3 is based on 50 simulations. Note that a 0 dB noise level corresponds to noise with the same mean amplitude (i.e. 1) as the Barker code. However, the noise persists throughout the signal at this level. 3 dB corresponds to a mean noise amplitude of 0.707 (power 0.5) and 6 dB to 0.5 (power 0.25)

Note also that a radar receiver needs an output SNR (i.e. $2E/N_0$) of 100 (20 dB), and

$$\frac{E}{N_0} = n(B\tau) \frac{S}{N}. \quad (5.12)$$

So the receiver needs

$$\frac{S}{N} = \frac{100}{n(B\tau)}. \quad (5.13)$$

In the above case, $n = 20$ and $B\tau = 13$, so the required $S/N = 0.38$, i.e. a mean-amplitude ratio of 0.62.

6. Methods for detection and identification of combined Barker sequences

6.1 Correlation/matched-filter techniques

Combined Barker sequences may be expressed as the Kronecker product of a pair of Barker sequences. This is worthwhile as the Matlab routine ‘kron’ may be used to produce combined sequences. The Barker sequences of lengths r and s may be represented by the vectors:

$$\begin{aligned} \mathbf{B}_r &= (\alpha_i) = (\alpha_1 \ \alpha_2 \ \dots \ \alpha_r) \\ \mathbf{B}_s &= (\beta_j) = (\beta_1 \ \beta_2 \ \dots \ \beta_s) \end{aligned} \quad (6.1)$$

A combined Barker sequence \mathbf{B}_{rs} is produced by the Kronecker product $\mathbf{B}_r \otimes \mathbf{B}_s$, i.e. taking $\mathbf{B}_s = (\beta_j)$ and replacing each entry β_j by the r -vector $\beta_j(\alpha_i)$:

$$\begin{aligned} \mathbf{B}_{rs} &= \mathbf{B}_r \otimes \mathbf{B}_s = (\gamma_k) \\ &= (\beta_1(\alpha_i) \ \beta_2(\alpha_i) \ \dots \ \beta_s(\alpha_i)) \\ &= (\beta_1\alpha_1 \ \beta_1\alpha_2 \ \dots \ \beta_1\alpha_r \ \beta_2\alpha_1 \ \beta_2\alpha_2 \ \dots \ \beta_2\alpha_r \ \dots \ \beta_s\alpha_1 \ \beta_s\alpha_2 \ \dots \ \beta_s\alpha_r) \end{aligned} \quad (6.2)$$

Correlating the combined Barker sequence \mathbf{B}_{rs} with the inner sequence \mathbf{B}_r produces the matched-filter output:

$$c_k = \frac{1}{r} \sum_{j=0}^{r-1} \alpha_{j+1} \gamma_{k+j} \quad (6.3)$$

Note that c_k produces β_j values every r -th value of k :

$$\begin{aligned} c_1 &= \frac{1}{r} \beta_1 (\alpha_1^2 + \alpha_2^2 + \dots + \alpha_r^2) \\ c_{1+r} &= \frac{1}{r} \beta_2 (\alpha_1^2 + \alpha_2^2 + \dots + \alpha_r^2) \\ &\vdots \\ c_{1+(s-1)r} &= \frac{1}{r} \beta_s (\alpha_1^2 + \alpha_2^2 + \dots + \alpha_r^2) \end{aligned} \quad (6.4)$$

As, $\forall i, \alpha_i = \pm 1 \Rightarrow \alpha_i^2 = 1$, all the (...) terms in (6.4) equal r , giving:

$$c_{1+jr} = \beta_{j+1}, \quad 0 \leq j \leq s-1 \quad (6.5)$$

For all other c_k terms:

$$k \neq 1 + jr \Rightarrow |c_k| \leq \frac{1}{r} \quad (6.6)$$

Thus, correlating every r -th value of (c_k) with the outer sequence B_s produces the maximum matched-filter output:

$$\begin{aligned}
cc_1 &= \frac{1}{s} \sum_{j=0}^{s-1} \beta_{j+1} c_{1+jr} \\
&= \frac{1}{s} \sum_{j=1}^s \beta_j^2, \quad \text{from 6.5} \\
&= 1, \quad \text{as } \beta_j^2 = 1
\end{aligned} \tag{6.7}$$

The above suggests a 2-dimensional search for the presence of B_{rs} in a sample. Successively searching for B_r and B_s is more efficient than directly searching for B_{rs} , i.e. for the presence of a repeating (γ_k) in the sample. Correlating with an r -length sequence and an s -length is clearly more efficient than correlating with one of length rs . Furthermore, it is possible to estimate r before going on to estimate s . Because of poor cross-correlation properties of some Barker sequences, initial correlation of the sample with an incorrect B_r may lead to a weak repeating pattern, increasing the likelihood of false identification.

6.1.1. Estimation of B_j components

For a particular B_r and sample $Y=(y_i)$, the following matched filter results:

$$c_k = \frac{1}{r} \sum_{j=0}^{r-1} \alpha_{j+1} y_{k+j}, \quad k \geq 1 \tag{6.8}$$

The first stage in estimating the outer sequence is to correlate alternative B_s with c_k values at k -intervals of r , producing the cc_k^s sequence (matched-filter output):

$$cc_k^s = \frac{1}{s} \sum_{j=0}^{s-1} \beta_{j+1} c_{k+jr}, \quad k \geq 1 \tag{6.9}$$

If the correct B_s is used, the maximum value of 1 is produced when that B_s is aligned with identical r -spaced c values, as in (6.7), which happens once for each B_{rs} waveform (every M -th value of k in (6.9), $T = M\Delta t$). Thus, for noiseless (y_i) :

$$\max_k [cc_k^s] = 1 \tag{6.10}$$

and, for other k' :

$$|c_{k'+jr}| \leq \frac{1}{r} \quad \text{and} \quad \beta_j = \pm 1 \Rightarrow |cc_{k'}^s| = \left| \frac{1}{s} \sum_{j=0}^{s-1} \beta_{j+1} c_{k'+jr} \right| \leq \frac{1}{r} \tag{6.11}$$

Tests for B_s exploit the expected pulse train of 1's in cc_k^s for the correct s . The train of n pulses at intervals of $T (=M\Delta t)$, beginning at mT , may be represented:

$$\sum_{i=m}^{m+n-1} \delta(t - iT) = \text{rect} \left\{ \frac{t - t_0}{nT} \right\} \sum_{i=-\infty}^{\infty} \delta(t - iT) \quad (6.12)$$

$$t_0 = \left(m + \frac{n-1}{2} \right) T$$

Its Fourier transform is:

$$\text{FT} \left\{ \sum_{i=1}^{m+n-1} \delta(t - iT) \right\} = n e^{-j2\pi f t_0} \text{sinc}(nTf) * \sum_{i=-\infty}^{\infty} \delta \left(f - \frac{i}{T} \right) \quad (6.13)$$

Its amplitude spectrum is thus:

$$|\text{FT}\{ \} | = n |\text{sinc}(nTf)| * \sum_{i=-\infty}^{\infty} \delta \left(f - \frac{i}{T} \right), \quad (6.14)$$

i.e. a series of absolute sinc functions centred on frequencies 0 Hz, $\pm \frac{1}{T}$ Hz, $\pm \frac{2}{T}$ Hz

etc. The sinc centred on 0 Hz has zero values at frequencies $\pm \frac{1}{nT}$, $\pm \frac{2}{nT}$ Hz etc,

where $\frac{1}{nT} \ll \frac{1}{T}$. Tests for B_s may thus be based on the amplitude spectrum of cc_k^s - a phase independent test, i.e. m -independent.

An alternative and simpler test estimates M by taking average of cc_k^s values at p -intervals of k . Different values for p are tried within the likely range for M , which may be derived by examining the amplitude spectrum of cc_k^s as above, or may be known a priori. The p -interval averages are:

$$ccs_i^p = \frac{1}{L_p} \sum_{j=0}^{L_p-1} cc_{i+jp}^s, \quad L_p \leq \frac{N}{p} \quad (6.15)$$

where N is the number of available y samples. The largest of the p possible values ($i = 1, 2, \dots, p$) is taken for each possible p and the overall maximum over p is compared with a threshold to detect s :

$$\max_{p, 1 \leq i \leq p} [ccs_i^p] \geq \text{threshold} ? \quad (6.16)$$

A final alternative is to test the series resulting from taking every r -th value of the c_k in (6.8) using the techniques of section 5, i.e. test for a true Barker code.

Tests for a single true Barker code or a combined Barker code in the sample may be combined. Using an initial B_r matched filter may result in a pulse train of 1's or a recurring pattern associated with a further B_s . Thus it is possible to decide there is just a repeating true Barker code B_r present or go on to detect the additional B_s of a combined code.

6.1.2. Effects of additive Gaussian noise

Applying the matched filter of (6.8) to a sample consisting of a signal (x_i) in Gaussian noise (n_i):

$$y_i = x_i + n_i, \quad (6.17)$$

where n_i are independent samples from a zero-mean Gaussian distribution of variance σ^2 , produces

$$\begin{aligned} c_k &= \frac{1}{r} \sum_{j=0}^{r-1} \alpha_{j+1} (x_{k+j} + n_{k+j}) \\ &= \frac{1}{r} \sum_{j=0}^{r-1} \alpha_{j+1} x_{k+j} + \frac{1}{r} \sum_{j=0}^{r-1} \alpha_{j+1} n_{k+j} \end{aligned} \quad (6.18)$$

As $\alpha_{j+1} = \pm 1$, the noise in c_k has zero-mean and variance σ^2/r . This effect is repeated for cc_k^s in (6.9), which has a variance of σ^2/rs . This clearly aids detection, particularly for longer sequences, as does the smaller value for cc when β_j is not perfectly aligned (6.11).

6.2 Simulation results for matched filter/correlation techniques

As an illustration, identification rates are given for $B_{5,3}$ and $B_{13,7}$. c_k and cc_k^s were calculated as in (6.8, 6.9) and tests for B_s used (6.15). M was assumed to be in the range 600-800, when the actual value was 700.

Noise	% Identification	% False identification	% Failure to identify
6 dB	84	13	11
3 dB	81	14	16
0 dB	70	23	27

Table 6.1: Identification rates for $B_{5,3}$

Noise	% Identification	% False identification	% Failure to identify
6 dB	91	17	7
3 dB	88	21	10
0 dB	79	34	21

Table 6.2: Identification rates for $B_{13,7}$

Each estimated % in tables 6.1 and 6.2 is based on 100 simulations, with the same noise assumptions as described in 5.2.

Clearly, identification is better for the longer $B_{13,7}$, as expected, but false identification is also higher due to higher cross-correlations for the constituent Barker codes.

7. Alternative methods for Barker sequence detection

7.1 Neural network detection

Neural networks have previously been trained to recognize particular codes [5]. The current investigation has focussed on a 3-layer perceptron network with 13 input elements trained to detect B_{13} . The output layer has one neuron, which may be shown to give a sufficient statistic. All neurons in the hidden and output layers use a sigmoid function, and neuron thresholds are zero.

Sequence	Training input												
1	0	0	0	0	0	0	0	0	0	0	0	0	0
2	1	0	0	0	0	0	0	0	0	0	0	0	0
3	-1	1	0	0	0	0	0	0	0	0	0	0	0
4	1	-1	1	0	0	0	0	0	0	0	0	0	0
5	-1	1	-1	1	0	0	0	0	0	0	0	0	0
.													
.													
.													
13	1	1	1	1	-1	-1	1	1	-1	1	-1	1	0
14	1	1	1	1	1	-1	-1	1	1	-1	1	-1	1
15	0	1	1	1	1	1	-1	-1	1	1	-1	1	-1
.													
.													
.													
24	0	0	0	0	0	0	0	0	0	0	1	1	1
25	0	0	0	0	0	0	0	0	0	0	0	1	1
26	0	0	0	0	0	0	0	0	0	0	0	0	1

Table 7.1: Training set, without noise, for B_{13}

Training was carried out with the 26 possible sequences in Table 7.1 with additive noise, to attempt to get output 1 for sequence 14 and 0 for all other sequences.

[5] has shown that after training with noiseless codes, the signal-to-sidelobe ratio of this kind of network can achieve 42.7 dB for B_{13} and 49.7 dB for the 63-bit m-sequence, much higher than the respective 17 dB and 22 dB for matched filters. The neural network also performed much better in the presence of non-Gaussian noise. Current results so far for B_{13} with additive Gaussian noise have achieved around 35 dB, still a much superior detector to the conventional matched filter.

Future work will investigate the effects of the number of neurons in the hidden layer and alternative learning algorithms. Clearly, different networks would be needed for different codes, and subsequent analysis required to determine other parameters, e.g. T (or n). An obvious disadvantage of neural networks is their computational complexity.

7.2 Methods derived from CDMA multiuser detection

The pulse-compression technique in phase-coded radar involves the transmission of a long-duration wide-bandwidth signal code, properties shared by CDMS transmissions. Thus more severe problems arise when interfering CDMA signals are present. In these cases, it may be beneficial to use a modified multiuser detector (MUD), designed to reject multiple access interference (MAI) in CDMA, possibly blindly and adaptively. MUDs use information about all users' codes to cancel MAI, i.e. all users' signals except the wanted user's: in general, the more information used the better, and slower, the detection. In this application, *all users* constitute the MAI and the radar signal the desired user. MUDs using subspace methods [6] will be investigated: the basis of this approach is that, by performing an eigendecomposition of the autocorrelation matrix of signal samples, the signal is separated into radar signal and CDMA user subspace and the noise subspace.

MUDs exploiting the cyclostationarity and resulting high degree of spectral correlation of signals will also be investigated. Silent periods between pulse trains may be exploited to derive the (cyclostationary) CDMA interference model, removing the need for training sequences [7].

7.3 Independent component analysis (ICA)

This is a statistical technique which is suitable for blind estimation and detection when signals from multiple sensors are available. ICA finds a linear transformation of the signal vector to separate it into its component, statistically independent, parts. Phase-coded radar signals, any CDMA users' signals present, and noise will be mutually independent. The following model is assumed for the signal vector y :

$$y = Mx + n \quad (7.1)$$

where x is a vector containing the radar signal and CDMA users' signals, M is a mixing matrix, and n an additive noise vector. ICA computes a linear transform W such that the elements of

$$s = Wy \quad (7.2)$$

are as statistically independent as possible: these s -elements are estimates of the independent source signals, i.e. the radar and CDMA users' signals.

ICA has been used as a MUD for CDMA with little knowledge of even the wanted signal [8], and also for separating monopulse radar signals [9].

8. Conclusions and future work

Only the simple, low-complexity correlation and matched-filter methods of sections 5 and 6 have been investigated in detail. They produce good detection and identification rates for true Barker codes, less good for combined Barker codes. Further investigation into the cross-correlation properties of true Barker codes is needed to derive theoretical performance limits. It seems unlikely that the slightly improved performance of more sophisticated methods like neural networks would justify the extra complexity. Neural networks are not real-time methods for this application.

The techniques of section 6 may in principle be extended to analyse signals employing Barker-like codes constructed from three true Barker codes, $B_u \otimes B_v \otimes B_w$. E.g $B_{13} \otimes (B_{11} \otimes B_7)$ and $(B_{13} \otimes B_{11}) \otimes B_7$ are codes of length 1001. However, the properties of such codes are unknown and need investigation.

Finally, alternative noise environments need to be explored, in particular modified MAI techniques to cancel interfering signals.

9. References

1. E Hollis: Comparison of combined Barker codes for coded radar use, IEEE Trans Aerospace Electron Sys, AES-3/1, pp 141-143, 1967.
2. F E Nathanson: Radar Design Principles, McGraw Hill, 1969.
3. N Chang and S W Golomb: On n -phase Barker sequences, IEEE Trans on Information Theory, Vol 40/4, pp 1251-1253, 1994.
4. M Frieese: Polyphase Barker sequences up to length 36, IEEE Trans on Information Theory, 42/4, pp 1248-1250, 1996.
5. H K Kwan and C K Lee: A Neural Network Approach to Pulse Radar Detection, IEEE Trans on Aerospace and Electron Sys, 29/1, pp 9-21, 1993.
6. X Wang and H V Poor: Blind Multiuser Detection: a Subspace Approach, IEEE Trans on Information Theory, Vol 44, pp 677-691, 1998
7. S S H Wijayasuriya et al: A Novel Interference Rejection Scheme for DS-CDMA Using Adaptive Noise Cancellation, ICCS'94, pp 364-358, 1994.
8. T Ristaniemi and J Joutsensalo: Independent Component Analysis With Code Information Utilization in DS-CDMA Signal Separation, IEEE Globecom'99, Part A, pp 320-324, 1999.
9. E Chaumette, P Comon and D Muller: ICA-based Technique for Radiating Sources Estimation: Application to Airport Surveillance, IEE Proc-F, Vol 140/6, 1993.

10. Glossary

10.1 Abbreviations

ACF	autocorrelation function
CDMA	code division multiple access
CW	continuous wave
DFT	discrete Fourier transform
FFT	fast Fourier transform
ICA	independent component analysis
MAI	multiple-access interference
m-sequence	maximal-length sequence
MUD	multi-user detector
RF	radio frequency

10.2 Symbols

B	bandwidth
B_n	Barker code of length n
$B_{n,m}$	combined Barker code from B_n and B_m
c	velocity of light
C_m	ACF value for shift m
CC_j	Cross-correlation function value for shift j
E	input energy, i.e. $\bar{S}t_0$ (\bar{S} is the mean input signal power)
m	metres
n	number of pulses in train
N	noise input to receiver, i.e. N_0B
N_0	input-noise power spectral density (one-sided)
R	range to target
ΔR	range resolution
R_u	maximum unambiguous range
s	seconds
S	input signal power
t_0	length of pulse train
t_d	time delay
Δt_d	time-delay resolution
T	pulse-repetition interval
T_s	interval between pulse trains
τ	pulse duration
Ω	solid angle of search
Ω_b	solid angle of radar beam
\cong	approximately equal to
$*$	convolution
\otimes	Kronecker product, e.g. $(a_1 \ a_2) \otimes (b_1 \ b_2) = (b_1a_1 \ b_1a_2 \ b_2a_1 \ b_2a_2)$